Iranian Journal of Basic Medical Sciences
ijbms.mums.ac.ir

Intranasal administration of spike-specific mRNA-LNP confers more protection than the intramuscular route against SARS-CoV-2

Mohsen Abdoli [1], Hoorieh Soleimanjahi [1]*, Sara Soudi [2], Asghar Abdoli [3]

[1] Department of Virology, Faculty of Medical Sciences, Tarbiat Modares University, Tehran, Iran
[2] Department of Immunology, Faculty of Medical Sciences, Tarbiat Modares University, Tehran, Iran
[3] Department of Hepatitis and AIDS, Pasteur Institute of Iran, Tehran, Iran

ARTICLE INFO

Article type:
Original

Article history:
Received: Jan 31, 2026
Accepted: Jun 22, 2026

Keywords:
COVID-19 vaccines
Intranasal administration
Lipid Nanoparticles
mRNA vaccines
Mucosal immunity
SARS-CoV-2

ABSTRACT

Objective(s): Intranasal vaccination mimics natural infection and induces mucosal immunity against respiratory viruses. This study compared the immunogenicity and protective efficacy of a nucleoside-modified messenger RNA (mRNA) encoding the SARS-CoV-2 spike protein, encapsulated in lipid nanoparticles (LNPs), administered via intranasal (I.N) versus intramuscular (I.M) routes.

Materials and Methods: BALB/c mice received mRNA-LNP vaccines at 1, 5, or 10 µg doses intramuscularly. Antibody responses (Immunoglobulin G/IgA [IgG/IgA]), neutralization titers (conventional virus neutralization test [cVNT]), and interferon-gamma (IFN-γ) responses were assessed to select the optimal dose. The selected 5 µg dose was then administered to mice and Syrian hamsters via I.N or I.M routes. Post-challenge, lung viral loads (50% Tissue Culture Infectious Dose [$TCID_{50}$]/ml) and weight changes were evaluated.

Results: The 5 µg dose induced robust humoral and cellular immunity (cVNT >5 log_2). Intranasal delivery elicited strong spike-specific IgA in nasal washes. Although I.M vaccination produced higher serum neutralizing titers (51.2 vs. 22.0), I.N vaccination conferred superior protection with a 4-log reduction in lung viral load (~10^1 $TCID_{50}$/ml) versus I.M and controls (~10^2 $TCID_{50}$/ml). I.N-vaccinated hamsters were completely protected from weight loss, whereas I.M-vaccinated animals showed mild weight reduction (~1%).

Conclusion: Intranasal mRNA-LNP administration elicits potent mucosal and systemic immunity and provides superior protection against SARS-CoV-2 challenge compared to I.M vaccination, underscoring its promise as a transformative strategy for respiratory virus vaccines.

▶ Please cite this article as:
Abdoli M, Soleimanjahi H, Soudi S, Abdoli A. Intranasal administration of spike-specific mRNA-LNP confers more protection than the intramuscular route against SARS-CoV-2. Iran J Basic Med Sci 2026; 29:

Introduction

Coronavirus disease 2019 (COVID-19) emerged as a new disease caused by infection with severe acute respiratory syndrome coronavirus-2 (SARS-CoV-2). The COVID-19 pandemic has had a profound global impact, resulting in millions of deaths and overwhelming healthcare systems (1). SARS-CoV-2 is an enveloped, positive-sense single-stranded RNA (ssRNA) virus in the family *Coronaviridae*, genus *Betacoronavirus* (2). The first open reading frames (ORFs) of SARS-CoV-2 encode four major viral structural proteins: spike (S), membrane (M), envelope (E), and nucleocapsid (N) (3). Among these, the S protein facilitates viral entry into the host cell. It is well established that the virus uses its S protein to bind to the host cell receptor angiotensin-converting enzyme 2 (ACE2) (4). This interaction occurs between the receptor-binding domain (RBD) in the S1 subunit of the spike and the ACE2 receptor on the host cell surface. Consequently, the S protein is considered a major vaccine antigen (5).

Vaccines are central to the prevention, control, and even eradication of infectious diseases and are considered a cornerstone of healthcare systems nationally and internationally (6). Various platforms have been pursued simultaneously for COVID-19 vaccine development, including inactivated and live-attenuated virus vaccines, subunit vaccines, virus-like particles, recombinant protein vaccines, viral vector vaccines (e.g., adenoviral and influenza virus vectors), and nucleic acid-based (mRNA and DNA) vaccines (7). Among these, the rapid development and exceptional efficacy of mRNA technologies propelled them to prominence in the COVID-19 vaccine race. This is primarily because the technology requires only the viral genome sequence, rather than a live virus, and can be designed within days. Moreover, cell-free vaccine production is relatively straightforward to scale up, thus offering an advanced tool for rapid intervention during epidemics and pandemics (8). During the SARS-CoV-2 pandemic, most vaccines granted emergency use authorization by the FDA were administered intramuscularly. This route primarily elicits systemic immunity, whereas local and mucosal immunity are pivotal for hindering viral attachment and shedding in the respiratory tract (9). COVID-19 intranasal

***Corresponding author:** Hoorieh Soleimanjahi. Department of Virology, Faculty of Medical Sciences, Tarbiat Modares University, Tehran, Iran. Tel/Fax: +98-2182883561, Email: soleim_h@modares.ac.ir

(IN) vaccines have shown a promising ability to elicit robust antibody-mediated and cell-mediated immune responses. Additionally, they have the added advantage of stimulating protective mucosal immunity and offer greater ease of administration than intramuscular vaccines (10). Thus, the route of administration can play a key role in controlling virus shedding, transmission, and the emergence of new variants during a pandemic.

One of the most essential advantages of mRNA vaccines is the ease and speed of production. The rationale behind mRNA vaccination is straightforward: once the target immunogen is selected, its sequence can be rapidly synthesized. This process is scalable, cell-free, and requires minimal alteration during formulation and mRNA synthesis (11). Second, mRNA vaccines enable rapid production of target antigens upon transfection and translation in host cells. Since translation occurs in the cytoplasm, mRNA vaccines offer higher biosafety than DNA vaccine candidates (12). Furthermore, mRNA is non-integrating and does not incorporate into the host cell's DNA. Unlike traditional protein-based vaccines produced in bacterial systems, mRNA vaccines utilize the host's translation machinery. Consequently, the generated antigens closely resemble viral proteins in structure, including any necessary post-translational modifications for proper antigen function (13).

Although mRNA vaccines are highly efficacious, they have limitations, including reduced stability and a requirement for stringent cold-chain storage. Lipid nanoparticles (LNPs) address these challenges by providing a protective environment for mRNA molecules and facilitating efficient intracellular delivery (8). LNPs are currently the most advanced delivery system for mRNA. They are composed of four distinct lipid components: an ionizable lipid, a helper phospholipid, cholesterol, and a PEGylated lipid (14). These lipids self-assemble into nanosized particles via methods like ethanol dilution. The synthesis process is critical as it directly determines the physicochemical properties of the LNPs, including size, charge, encapsulation efficiency, and transfection capability (15). According to common LNP synthesis protocols, mRNA is solubilized in an aqueous phase and encapsulated via a condensation method, or complexed with preformed LNPs in a second step (16). The Pfizer-BioNTech COVID-19 vaccine and the candidate developed by CureVac are both based on LNP technology developed by Acuitas Therapeutics (17).

While mRNA-LNPs have proven effective via intramuscular injection, this route primarily induces systemic immunity, offering limited protection against initial infection and shedding at the respiratory mucosa (9, 10). Intranasal vaccination presents a compelling alternative, as it directly targets the nasal-associated lymphoid tissue (NALT), potentially inducing sterilizing mucosal immunity that could neutralize the virus at its point of entry, reduce transmission, and provide broader protection against emerging variants (9). Although the promise of intranasal mRNA vaccines is recognized, direct comparative studies of identical mRNA-LNP formulations administered intranasally versus intramuscularly are still needed to unequivocally demonstrate the superiority of mucosal delivery in relevant animal models. In this study, we developed a SARS-CoV-2 spike-encoding mRNA-LNP vaccine. We performed a head-to-head comparison of its immunogenicity and protective efficacy following intranasal versus intramuscular administration in mice and hamsters. We demonstrate that intranasal delivery, while generating slightly lower systemic antibody titers, induces potent mucosal IgA and confers significantly superior protection upon viral challenge, nearly abrogating viral replication in the lungs.

Materials and Methods

Ethics statement

The animal study procedures were reviewed and approved by the Animal Ethics Committee of Tarbiat Modares University (IR.MODARES.REC1401.085). All mouse experiments were performed in accordance with relevant guidelines and regulations, including the ARRIVE guidelines. Veterinary best practices were followed for anesthesia and euthanasia, as recommended by the American Veterinary Medical Association (AVMA) Guidelines for the Euthanasia of Animals (2020). The animals were anesthetized via injection of a cocktail of 10% ketamine and 2% xylazine. The animals were maintained under conventional conditions, with the temperature set at 25 °C and a controlled light cycle of 12 hr light/12 hr darkness. The animals were fed a regular diet and water *ad libitum*.

Spike-specific mRNA and LNP production process

A sequence-optimized mRNA encoding the full-length SARS-CoV-2 S protein was synthesized and purified in vitro as previously described (18). Briefly, appropriate amounts of lipids—including the ionizable lipid SM-102 (Avanti Polar Lipids, USA), 1,2-distearoyl-sn-glycero-3-phosphocholine (DSPC, Avanti Polar Lipids, USA), cholesterol (Avanti Polar Lipids, USA), and 1,2-dimyristoyl-rac-glycero-3-methoxypolyethylene glycol-2000 (DMG-PEG2000, Avanti Polar Lipids, USA)—were mixed in ethanol at molar ratios of 50:10:38.5:1.5, respectively. The lipid mixture was then combined with an mRNA-containing sodium acetate buffer at a 3:1 ratio (aqueous:ethanol) using a microfluidic T-mixer. The resulting mRNA-LNPs were diluted with Tris buffer (pH 7.4) containing sucrose, underwent buffer exchange, and were concentrated via tangential flow filtration. The formulation was sterile-filtered (0.22 μm) and stored at -20 °C or 2–8 °C for subsequent use. Empty LNPs were synthesized using an identical method, omitting mRNA from the aqueous solution. Finally, the prepared LNPs were stored at 4°C after buffer exchange and concentration in Tris buffer (pH 7.4) (19).

Nanoparticle characterization

The hydrodynamic diameter, polydispersity index (PDI), and zeta potential of the mRNA-LNPs were analyzed using dynamic light scattering (DLS) with a ZetaSizer Nano instrument (Malvern Instruments, UK). Measurements were performed in triplicate at a 1:100 dilution in a 10 mM NaCl solution at 25 °C.

Encapsulation efficiency

The encapsulation efficiency was assessed using fluorescence spectroscopy, with fluorescence intensities converted to mRNA concentrations. A series of eight mRNA solutions (1000, 500, 250, 125, 62.5, 31.25, 15.625, and 0 ng/ml) was prepared in Tris-EDTA buffer. mRNA-LNPs were also dissolved in Tris-EDTA buffer to obtain a sample with an approximate mRNA concentration of 250 ng/mL. Additional samples were prepared under the same buffer conditions but with 0.5% Triton-X100 added. Then, 100 μl of

Table 1. Immunization schedule and experimental groups for dose optimization of a SARS CoV 2 spike encoding mRNA lipid nanoparticle (LNP) vaccine in BALB/c mice

Mice groups BALB/c	Immunization		Administration method	Number
	First dose (Day zero)	Second dose (Day 21)		
Low Dose groups	1 µg mRNA-S	1 µg mRNA-S	Intramuscular	7
Medium Dose groups	5 µg mRNA-S	5 µg mRNA-S	Intramuscular	7
High Dose groups	10 µg mRNA-S	10 µg mRNA-S	Intramuscular	7
Negative control groups	50 µl PBS	50 µl PBS	Intramuscular	7
Adjuvant group (nanoparticles)	50 µl LNP	50 µl LNP	Intramuscular	7
Optimal dose	5 µg mRNA-S	5 µg mRNA-S	Intranasal	7

LNP: Lipid nanoparticles

each standard and sample solution was transferred into the wells of a 96-well plate, followed by the addition of 100 µl of 50 µM SYBR Green II. After a 5-minute incubation period, fluorescence intensity was measured using a fluorescence plate reader at excitation and emission wavelengths of 490 nm and 520 nm, respectively. A calibration curve generated from the mRNA solutions was used to convert fluorescence readings into mRNA concentrations. The fluorescence measured from mRNA-LNP samples in Tris-EDTA buffer containing Triton-X100 was taken as the total mRNA content. In contrast, the sample from plain Tris-EDTA buffer represented the free (unencapsulated) mRNA. Finally, the encapsulation efficiency (%EE) was calculated using equation (1), where W(total) denotes the initial mRNA concentration and W(free) refers to the concentration of encapsulated mRNA (20).

$$\%EE = \frac{W(total\ mRNA) - W(free\ mRNA)}{W(total\ mRNA)} \times 100 \quad (1)$$

Experimental vaccination of mRNA/ LNPs in mice and hamsters

All animal procedures were reviewed and approved by the Animal Ethics Committee of Tarbiat Modares University. A total of 42 female BALB/c mice, aged six to eight weeks and weighing approximately 20 g each, were used in this experiment. All animals were housed under standard conditions with ad libitum access to food and water. At the end of the experimental period, animals were humanely euthanized for sample collection. Mice were euthanized using CO_2 inhalation followed by cervical dislocation as a secondary method to ensure death. The immunization schedule for intramuscular administration is presented in Table 1. The mice were randomly assigned to five groups (n=7). On day zero, LNPs containing 1 µg (low dose), 5 µg (medium dose), or 10 µg (high dose) of mRNA were administered intramuscularly. Two additional groups served as controls, receiving either PBS (negative control) or empty LNPs (adjuvant control). At the end of this phase, the optimal dose was selected based on measured levels of anti-spike IgG, IFN-γ, and neutralizing antibodies. This selected dose was then administered to a separate group of mice (n=7) intranasally to assess the level of protection. For intramuscular administration, a 50 µl volume of each vaccine candidate was injected into female BALB/c mice. For intranasal administration, mice were anesthetized via intraperitoneal injection of ketamine (100 mg/kg) and xylazine (10 mg/kg), and a total volume of 50 µl of the vaccine candidate was administered, with 25 µl delivered into each nostril.

A total of 40 female Syrian golden hamsters (6–7 weeks old) were obtained from the Pasteur Institute of Iran and housed under standard laboratory conditions. Animals were randomly divided into four experimental groups (n=10 per group). Two groups were immunized with the optimal dose of 5 µg mRNA-LNPs, administered either intranasally or intramuscularly, in a two-dose regimen on days 0 and 21 (Table 2). The remaining two groups served as adjuvant controls, receiving empty nanoparticles (without mRNA) via either the intranasal or intramuscular route. All vaccine formulations were delivered in a final volume of 50 µl per dose, consistent across both delivery routes and animal models (mice and hamsters). Prior to intranasal administration, all hamsters were anesthetized using a combination of ketamine (100 mg/kg) and xylazine (10 mg/kg) administered intraperitoneally (21, 22). Intramuscular injections were administered into the quadriceps muscle without anesthesia. For sample collection, hamsters were euthanized via an intraperitoneal overdose injection of ketamine (300 mg/kg) and xylazine (15 mg/kg), in compliance with institutional ethical guidelines for animal care and use.

Evaluation of spike-specific IgG antibody

Three weeks post-immunization, blood was collected from five mice per group via the retro-orbital plexus under anesthesia to assess IgG titers. For blood collection, mice

Table 2. Immunization and viral challenge protocol for protective efficacy assessment of the selected 5 µg dose of SARS CoV 2 spike encoding mRNA lipid nanoparticle (LNP) vaccine in Syrian golden hamsters

Hamster groups	Immunization		Administration method	Number
	First dose (Day zero)	Second dose (Day 21)		
Selected dose	5 µg mRNA-S	5 µg mRNA-S	Intranasal	10
Selected dose	5 µg mRNA-S	5 µg mRNA-S	Intramuscular	10
Adjuvant group (nanoparticles)	50 µl LNP	50 µl LNP	Intranasal	10
Adjuvant group (nanoparticles)	50 µl LNP	50 µl LNP	Intramuscular	10

LNP: Lipid nanoparticles

were placed under general anesthesia via intraperitoneal injection of a freshly prepared ketamine/xylazine cocktail (80–100 mg/kg ketamine and 5–10 mg/kg xylazine in sterile saline). The anesthetic mixture was administered at a volume not exceeding 10 ml/kg body weight. The absence of a pedal withdrawal reflex and a stable respiratory rate confirmed the depth of anesthesia. Each animal was gently restrained by scruffing while the head was stabilized. Using a sterile micro-hematocrit capillary tube, the tip was inserted at a 45° angle through the conjunctiva at the medial canthus to access the retro-orbital venous sinus, taking care to avoid injury to the eye. Approximately 0.2 ml of blood was collected into a microtube. Mice were closely monitored post-procedure for signs of trauma or distress before being returned to their cages. The procedure was performed using strict aseptic technique and adhered to institutional animal care and use guidelines. Blood samples were allowed to clot at room temperature for 1 hr, then incubated at 4 °C for at least 5 hr to ensure complete clot retraction. Serum was separated by centrifugation at 290 × g for 10 minutes and stored at −20 °C until analysis. Individual serum samples were analyzed using an ELISA to quantify spike-specific IgG levels. For the assay, recombinant spike protein (Sina Biotechnology, Iran) was diluted in bicarbonate/carbonate coating buffer (100 mM, pH 9.6) to a final concentration of 1 µg/ml. A 100 µl volume of the diluted protein was added to each well of an ELISA plate and incubated overnight at 4 °C. The following day, wells were washed three times with PBS, and non-specific binding sites were blocked by adding 150 µl of blocking buffer containing 1% bovine serum albumin (BSA). After a 1-hr incubation at room temperature, serial dilutions of mouse sera prepared in PBS were added to the wells and incubated for 2 hr. Subsequently, a 1:1000 dilution of HRP-conjugated anti-mouse IgG (Sino Biological, China) was added and incubated for 1 hr. Tetramethylbenzidine (TMB) substrate and stop solution were then sequentially added, and absorbance at 450 nm was measured with an ELISA reader. All serum samples were tested in duplicate.

Evaluation of spike-specific IgA antibody

To measure IgA, the nasal cavities of anesthetized mice were gently flushed with PBS from the posterior opening of the nose, and the fluid was collected using a micropipette. The collected samples were centrifuged at 10,000 × g for 15 min to remove debris. The resulting supernatants were stored at −20 °C for later analysis. Spike-specific IgA antibodies were detected using an alkaline phosphatase-conjugated anti-IgA antibody (Sigma-Aldrich, USA). The reaction was developed by incubating the wells with an alkaline phosphatase substrate. Finally, the optical absorbance was measured at 450 nm after adding the stop buffer using an ELISA plate reader (23, 24).

Neutralizing antibody response in sera

The conventional virus neutralization test (cVNT) evaluates the ability of functional antibodies in the serum to neutralize the virus in cell culture. Virus cultivation and handling of wild-type virus were performed in a biosafety level 3 (BSL-3) laboratory. Virus neutralization assays were performed by incubating 50 µl of twofold serial dilutions of heat-inactivated serum (56 °C for 30 min; in triplicate) with an equal volume of 100 $TCID_{50}$ (50% tissue culture infectious dose) of SARS-CoV-2 at 37 °C with 5% CO_2 for 1 hr. Briefly, the 50 µl of twofold serial dilutions of the heat-inactivated sera were mixed with an equal volume of 100 $TCID_{50}$ of SARS-CoV-2. Next, the mixture was transferred onto monolayers of Vero cells (obtained from the Cell Bank of the Pasteur Institute of Iran, Tehran, Iran) in 96-well plates and incubated for one hour at 37 °C. To assess cytopathic effects (CPE), infected cells were incubated for 3 days at 37 °C. The virus neutralization titer was determined as the highest serum dilution that completely inhibited the appearance of CPE, as previously described (25).

Analysis of IFN-γ responses

Spleen cell suspensions were prepared via gentle homogenization. Red blood cells (RBCs) were lysed by incubation in RBC lysis buffer (20 mM Tris, 160 mM NH_4Cl, pH 7.4) for five minutes at room temperature. The splenocytes were then washed with RPMI 1640 (Bioidea, Iran) and resuspended at a density of 2×10^6 cells/ml in RPMI containing 10% fetal bovine serum (FBS), 2 mM L-glutamine, 100 µg/ml streptomycin, and 100 U/ml penicillin. The cells were transferred to flat-bottom 24-well plates (Nunc, Denmark), stimulated with 10 µg/ml spike protein (Sina Biotechnology Company, Iran), and incubated at 37 °C in a 5% CO_2 atmosphere. Culture supernatants were harvested at 72 hr, and IFN-γ levels were measured using an ELISA kit according to the manufacturer's instructions (Karmania Pars Gene, Iran). Concanavalin A and PBS were used as positive and negative controls, respectively.

Animal challenge

For immunization, ten hamsters per group received two doses of the candidate vaccine. Three weeks after the second dose (day 42), ten hamsters per group were challenged intranasally with 10^5 plaque-forming units (PFU) per 100 µl of SARS-CoV-2 (Wuhan strain, clinical isolate). Prior to viral challenge, blood samples were collected from the lateral tail vein of hamsters (6–8 weeks old) under mild restraint without anesthesia. Animals were gently placed in a restraining tube or held manually using a clean towel to minimize stress and movement. The tail was warmed using a warm compress, and after disinfection with 70% ethanol, the lateral tail vein was punctured using a sterile 27G insulin syringe at the distal third of the tail. A 350–500 µl volume of blood was collected from each animal into microtubes. Hemostasis was achieved by applying gentle pressure with sterile gauze to the puncture site. Animals were monitored briefly post-procedure and returned to their cages once fully recovered. Weight loss and mortality were monitored daily post-infection. Hamsters were monitored daily for body weight changes over 9 days following viral challenge. On day six post-challenge, five hamsters from each group were euthanized by intraperitoneal injection of ketamine (300 mg/kg) and xylazine (15 mg/kg). Lung tissues were subsequently harvested to determine viral titers using the $TCID_{50}$ assay, calculated via the Spearman-Kärber method. The remaining five hamsters in each group were monitored daily until day nine post-challenge to evaluate weight changes (26).

SARS-CoV-2 load in lungs post-challenges

Lung tissues were homogenized in sterile DMEM medium using a tissue homogenizer to ensure uniform sample preparation. The lung homogenates were clarified by centrifugation at 4000 × g for 10 min to remove cell debris, and the supernatants were stored at -80°C until analysis.

Vero cells at 80% confluency in 96-well plates were infected with serial ten-fold dilutions of the clarified lung samples in DMEM. After 72 hr of incubation at 37°C in a 5% CO_2 atmosphere, the cultures were observed for the cytopathic effect of SARS-CoV-2. The viral titer in each lung specimen was calculated by the Kärber method and expressed as the 50% tissue culture infective dose ($TCID_{50}$)/ml (27).

Statistical analysis

GraphPad Prism 8.12 (GraphPad Software Inc., San Diego, USA) was used for data analysis. The Mann-Whitney test and one-way ANOVA were used to compare serological and cell-mediated immunity among animal groups. Neutralizing antibody titers were analyzed using a non-parametric Spearman's correlation test. *P*-values<0.05 were considered statistically significant at a 95% confidence interval (95% CI).

Results

Nanoparticles characterization

Dynamic light scattering (DLS) analysis revealed a narrow size distribution for the mRNA-LNPs, indicating high particle uniformity. The average particle size was approximately 103 nm for unloaded LNPs and 173 nm for mRNA-loaded LNPs. The formulated LNPs exhibited a positive zeta potential, measuring +48.4 mV for empty LNPs and +25 mV for mRNA-encapsulated LNPs. Despite the expectation that ionizable lipids are predominantly neutral at physiological pH, both formulations exhibited a positive zeta potential. This can be explained by the partial protonation of SM102 at pH 7.4 (pKa ~ 6.68, resulting in ~16–20% positively charged headgroups), the adsorption of positively charged Tris cations (pKa ~ 8.1) onto the nanoparticle surface, and the net neutral character of the helper lipids, which do not introduce opposing negative charges. Additionally, the encapsulated mRNA is largely confined to the particle core, allowing the outer surface to retain a modest positive charge. Collectively, these factors account for the observed positive zeta potential, which reflects a dynamic equilibrium rather than permanent cationicity. A zeta potential of +20 to +30 mV indicates moderate to good colloidal stability, and the narrow distribution reflects good formulation consistency. The positive zeta potential values observed for both empty and mRNA-loaded LNPs indicate good colloidal stability, which helps prevent particle aggregation. The reduction in zeta potential following mRNA encapsulation (from +48.4 mV to +25 mV) suggests successful complexation of the negatively charged mRNA with the lipid components, partially neutralizing the surface charge. This shift is typical and supports effective mRNA loading within the nanoparticles. These characteristics indicate stable, monodisperse nanoparticles suitable for efficient mRNA delivery in therapeutic applications (Figure 1).

Encapsulation efficiency

The encapsulation efficiency of mRNA within LNPs was determined using a fluorescence-based method employing SYBR Green II. This dye exhibits strong fluorescence upon nucleic acid binding but remains weakly fluorescent in its free form. A standard curve was generated by measuring the fluorescence of serial dilutions of the same mRNA used to synthesize the mRNA-LNPs, following the addition of SYBR Green II dye, as detailed in the Methods section. The resulting calibration curve showed an excellent linear correlation between RNA concentration and fluorescence intensity ($R^2 = 0.980$). To quantify the total mRNA content, Triton X-100 was added to disrupt the LNP structure, releasing the encapsulated mRNA. The fluorescence signal from the intact nanoparticle sample represented

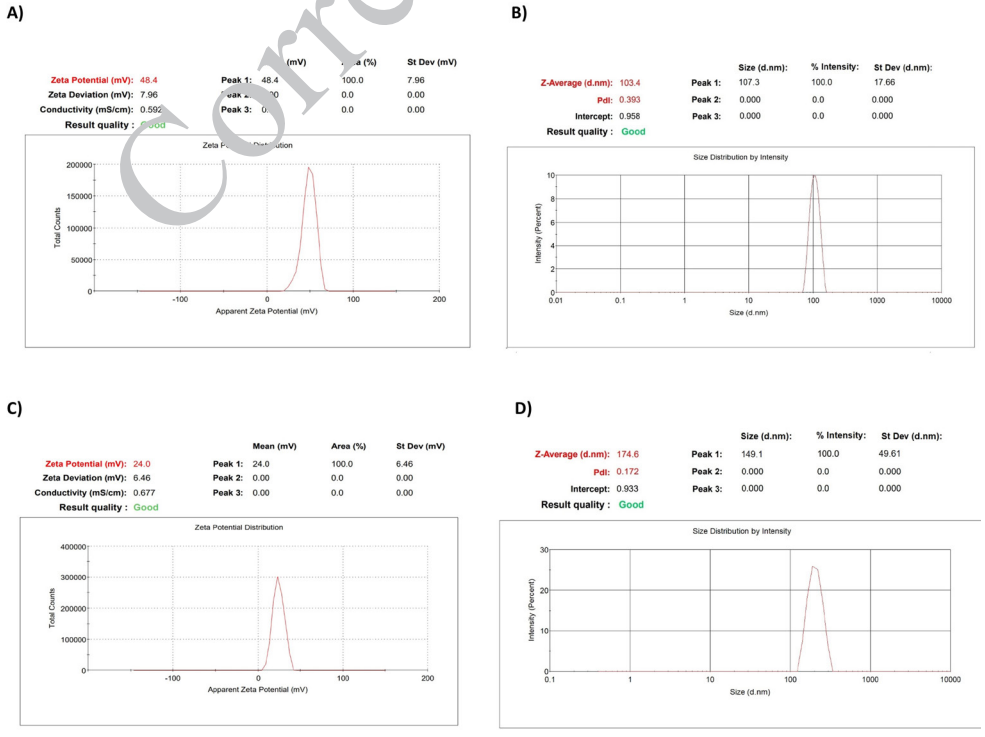

Figure 1. Nanoparticles characterization
A) Zeta potential of Unloaded Lipid Nanoparticles (LNPs), B) Hydrodynamic diameter of unloaded LNPs, C) Zeta potential of messenger RNA-Lipid Nanoparticles (mRNA-LNPs), D) Hydrodynamic diameter of mRNA-LNPs

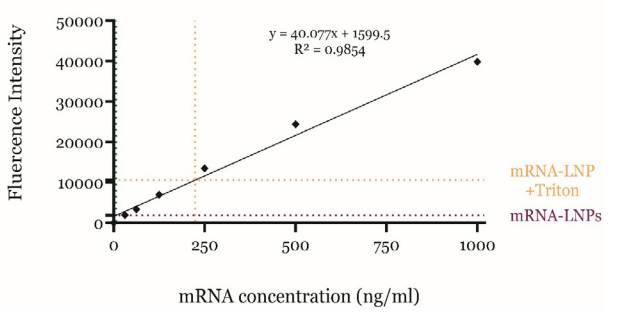

Figure 2. Quantification of mRNA encapsulation efficiency using SYBR Green II fluorescence assay

A standard curve was generated by plotting fluorescence intensity against serial dilutions of the same mRNA used for LNP synthesis, yielding a linear regression equation of y= 40.077x + 1599.5 with an R^2 value of 0.9854, indicating a strong correlation. Fluorescence signals from intact mRNA-LNPs (representing free, unencapsulated mRNA) and Triton X-100-disrupted mRNA-LNPs (representing total mRNA) are shown. The difference between these values was used to calculate the encapsulation efficiency.

LNP: Lipid Nanoparticle

free (unencapsulated) mRNA. The encapsulated mRNA concentration was then calculated by subtracting the free mRNA amount from the total mRNA. Encapsulation efficiency (%EE) was calculated using the following formula:

$$\%EE = (\text{Total mRNA} - \text{Free mRNA}) / \text{Total mRNA} \times 100$$

Using this approach, the mRNA-LNPs achieved an encapsulation efficiency of approximately 95% (Figure 2), which exceeds the generally accepted threshold of 80%. The corresponding calculation is shown below:

$$\%EE = (223.78\ \mu g - 6.87\ \mu g) / 223.78\ \mu g \times 100 = 95\%$$

Immunization with mRNA-LNP increases S-specific serum IgG antibody responses

The ability of the formulated spike-encoding mRNA-LNPs to induce a humoral immune response was assessed by ELISA (Figure 3). The results indicated a significant increase in anti-spike IgG antibody levels in the serum of mice that received the mRNA compared to the PBS and empty LNP control groups. Increasing the mRNA concentration from 1 µg to 5 µg significantly (P<0.0001) enhanced the IgG response, indicating a strong dose-dependent effect within this range. However, increasing the dose to 10 µg did not yield a statistically significant increase in the IgG response (P>0.05) compared with the 5-µg dose. This suggests that the immune response may reach a saturation point beyond which additional mRNA does not increase antibody production. This plateau effect is important for optimizing vaccine dosing, as it highlights the potential to achieve maximal immune responses without unnecessarily increasing the dose.

Administration of mRNA-LNP elicits cell-mediated cytokine

IFN-γ levels were measured as an indicator of Th1 polarization in splenocyte culture supernatants from immunized mice. As shown in Figure 4, mice immunized with mRNA-LNPs exhibited a relatively dose-dependent increase in IFN-γ secretion. The low, medium, and high mRNA dose groups showed significantly elevated IFN-γ levels of 553.8 pg/ml, 673.2 pg/mL, and 710 pg/mL, respectively, compared to the PBS control group (50.4 pg/mL) and LNP group (180.2 pg/mL) (P≤0.05). The high-dose

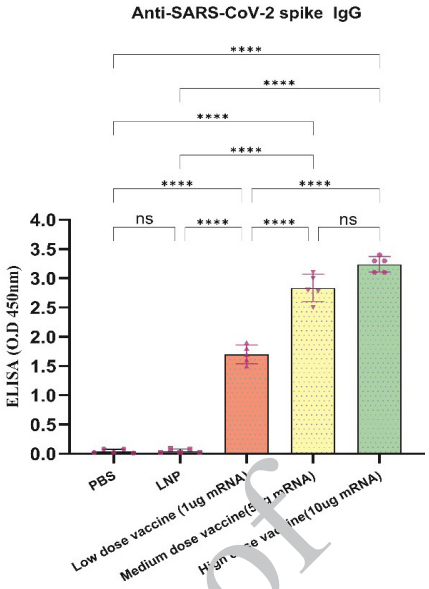

Figure 3. Serum spike-specific IgG response following immunization with spike-encoding mRNA-LNPs in mice

Female BALB/c mice (n=7 per group) were assigned to five experimental groups. They received a vaccine at mRNA doses of 1, 5, or 10 µg, PBS (as a negative control), and LNP via intramuscular injection. To assess the immune response, serum levels of Spike-specific IgG antibodies were quantified at a 1:1000 dilution using an ELISA kit. Each data point corresponds to an individual mouse. The data are presented as the mean ± standard error of the mean. Statistically significant differences were calculated using one-way ANOVA (significant differences are shown as ns: P>0.05, *: P<0.05, **: P<0.01, ***: P<0.001, ****: P<0.0001).

IgG: Immunoglobulin G, mRNA-LNPs: Messenger RNA-lipid nanoparticles, PBS: Phosphate buffered saline, ELISA: Enzyme-linked immunosorbent assay, NOVA: One-way analysis of variance

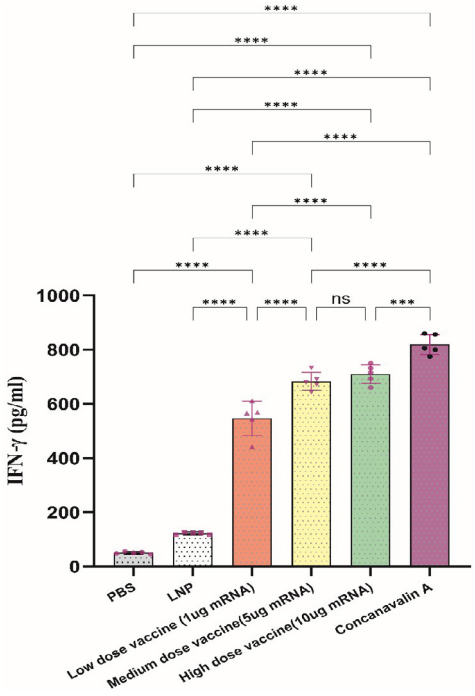

Figure 4. T-cell immune response in mRNA-LNPs immunized mice

Concentrations of the secreted Th1 cytokine IFN-γ were quantified using ELISA. Each data point corresponds to an individual mouse. The data are presented as the mean ± standard error of the mean. Statistically significant differences were calculated using one-way ANOVA (significant differences are shown as ns: P>0.05, *: P<0.05, **: P<0.01, ***: P<0.001, ****: P<0.0001).

mRNA-LNPs: Messenger RNA-lipid Nanoparticles, Th1: T-helper 1, IFN-γ: Interferon-gamma, ELISA: Enzyme-linked immunosorbent assay, ANOVA: One-way analysis of variance

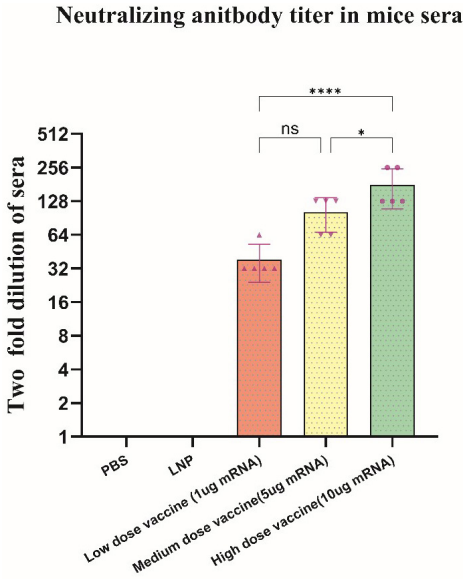

Figure 5. Neutralizing antibody titers test in control groups and groups receiving different vaccine doses in mice

Serum functional antibodies in the BALB/c mouse model with low (1 µg), medium (5 µg), and high (10 µg) vaccine doses were determined by Virus neutralization (VNT) assays test. Non-parametric Spearman's correlation test determined the neutralizing antibody titer. The neutralizing antibody titer equal to or larger than 32-fold (5 µg) was selected as a correlate of protection

mRNA-LNPs: Messenger RNA-lipid nanoparticles, PBS: Phosphate-buffered saline

group reached a level comparable to that of the concanavalin A-treated positive control group (823.8 pg/mL). Although both the medium- and high-mRNA dose groups exhibited elevated IFN-γ levels compared to the control groups, the difference between them was not statistically significant. Several factors may contribute to this plateau effect in the immune response at higher mRNA doses, including saturation of antigen-presentation pathways, a ceiling effect in immune stimulation, negative feedback mechanisms, potential innate immune activation, and limits on T cell clonal expansion. The results demonstrate that intramuscular immunization with spike-encoding mRNA-LNPs elicits a robust Th1-biased immune response, characterized by elevated IFN-γ secretion.

Immunization with mRNA-LNP leads to a rise in neutralizing antibody responses in immunized mice sera

Sera from mice immunized with 1 µg, 5 µg, and 10 µg mRNA-LNPs were analyzed for neutralizing antibody titers on day 42 post-immunization. Control groups received LNP or PBS. The PBS and LNP groups showed no detectable neutralizing activity. In contrast, mice receiving low, medium, and high doses of mRNA showed dose-dependent increases in neutralizing antibody titers, with mean values of 38.4, 102.4, and 179.2, respectively. These results indicate that increasing mRNA doses enhances the production of functional antibodies capable of virus neutralization. Sera from mice immunized with 5 µg and 10 µg mRNA showed more than a 5 $\log_2$ antibody titer compared to the control groups. This suggests that higher mRNA doses more effectively stimulate B cell activation and antibody affinity maturation, resulting in greater neutralizing capacity against the target antigen (Figure 5).

Although administering 10 µg mRNA resulted in the highest IgG, IFN-γ, and neutralizing antibody levels among the immunized mice, the difference between the 5 µg and 10 µg doses was not statistically significant for any of the immune responses evaluated. Given the lack of significant benefit at the higher dose and the potential for increased toxicity or adverse effects associated with higher mRNA concentrations, selecting the 5 µg dose appears to be a more prudent choice for vaccination. This approach balances immunogenic efficacy with safety, which is crucial for translational applications. This insight is important for optimizing vaccine dosing, indicating that increasing the mRNA dose beyond a certain point may not yield proportional immunological benefits but could instead increase cost or the risk of side effects.

Evaluation of mucosal IgA antibody

Based on the dose-optimization data, a group of mice (n = 7) received intranasal immunization with 5 µg of mRNA-LNPs, followed by a booster of 5 µg administered 21 days after the initial immunization. Three weeks after the intranasal booster immunization, nasal wash samples were collected, and the presence of spike-specific IgA antibodies was evaluated (Figure 6). Compared to the PBS (negative control) and empty LNP groups, mice that received the mRNA-LNP vaccine exhibited a significantly elevated IgA response ($P<0.0001$) in nasal secretions. The PBS and LNP groups showed negligible IgA levels, indicating minimal or no mucosal immune activation in the absence of spike-encoding mRNA. These findings demonstrate that intranasal administration of the optimized mRNA-LNP vaccine effectively induces a mucosal IgA immune response, which is crucial for neutralizing respiratory pathogens at the site of entry. The absence of a response in the control groups confirms the specificity of the vaccine-induced immunity. This mucosal IgA production may contribute to reduced viral colonization and transmission following respiratory

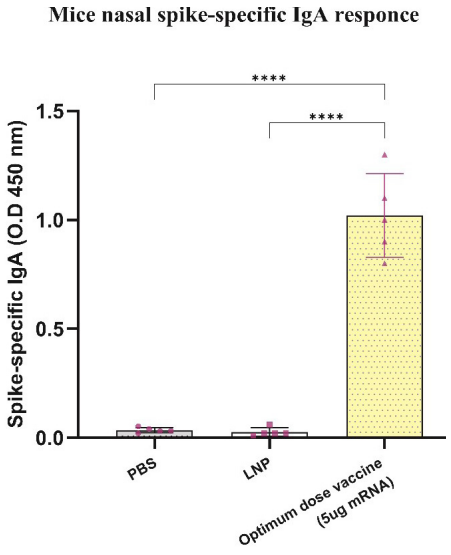

Figure 6. Local mucosal immune response following intranasal administration of the selected 5 µg vaccine dose against SARS-CoV-2 in mice. Anti-SARS-CoV-2 spike-specific IgA levels were measured by ELISA one week after the second intranasal immunization with 5 µg of the candidate mRNA-LNP vaccine. Each data point corresponds to an individual mouse. The data are presented as the mean±standard error of the mean. Statistically significant differences were calculated using one-way ANOVA (significant differences are shown as ns: $P>0.05$, *: $P<0.05$, **: $P<0.01$, ***: $P<0.001$, ****: $P< 0.0001$).

IgA: Immunoglobulin A, mRNA-LNP: Messenger RNA-lipid nanoparticle, ANOVA: One-way analysis of variance

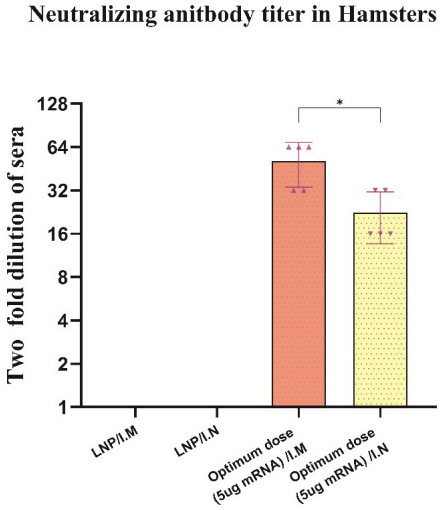

Figure 7. Neutralizing antibody titers in hamster sera following immunization with LNP or 5 µg mRNA vaccine formulations via I.M or I.N routes

Each data point corresponds to an individual mouse. The data are presented as the mean±standard error of the mean. Statistically significant differences were calculated using one-way ANOVA (significant differences are shown as ns: $P>0.05$, *: $P<0.05$, **: $P<0.01$, ***: $P<0.001$, ****: $P<0.0001$).

LNP: Lipid nanoparticles, I.M: Intramuscular, I.N : Intranasal

exposure. The optimized 5 µg dose was utilized to assess the protective efficacy of the vaccine candidate in subsequent viral challenge experiments conducted in female Syrian hamsters.

Intranasal mRNA-LNP vaccination limits viral shedding in the lung and reduces weight loss in hamsters

To assess the effectiveness of the mRNA-LNP vaccine in reducing viral shedding and lung viral titers, one group of hamsters (n=10) was immunized twice intranasally with the optimal mRNA dose (5 µg). In contrast, another group received the same dose via intramuscular injection. Additionally, two control groups received empty LNPs, either intranasally or intramuscularly. Three weeks following the second immunization, hamsters were intranasally challenged with 10^5 plaque-forming units (PFU) of SARS-CoV-2 in 100 µl. Six days after viral challenge, lung tissues were collected from five hamsters per group, and infectious viral titers were determined using the $TCID_{50}$/ml method. Before the challenge, serum samples were obtained to assess pre-challenge immune responses. The collected sera were analyzed for neutralizing antibody titers using a previously described method. The group receiving the optimum dose (5 µg mRNA) intramuscularly showed the highest neutralizing antibody titer, with a mean value close to 51.2, while the group receiving the optimum dose intranasally had a lower mean titer of approximately 22. As demonstrated in the preceding mouse experiments (Figure 5), neither empty LNPs nor PBS induced detectable neutralizing antibodies. Therefore, only empty LNPs were employed as the negative control in the hamster study to minimize animal use. As expected, the LNP/I.M and LNP/I.N groups (without mRNA) showed negligible or undetectable neutralizing antibody titers, confirming that the mRNA component is necessary for immunogenicity. Immunization with the optimal dose (5 µg mRNA) induced strong neutralizing antibody responses in hamsters, with intramuscular administration yielding slightly higher titers than intranasal administration (Figure 7).

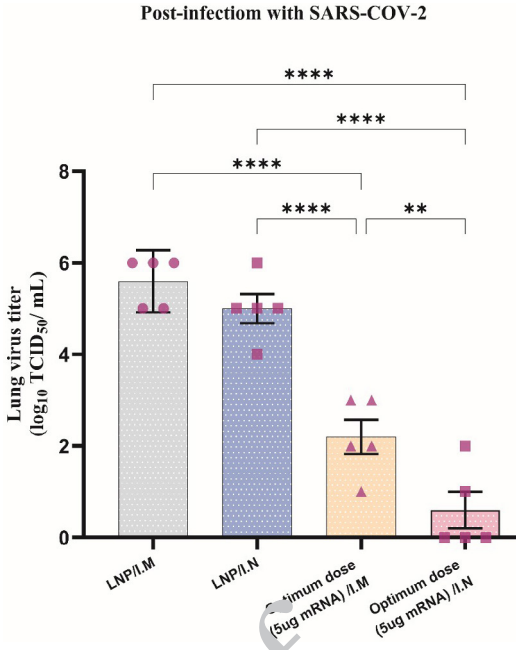

Figure 8. mRNA/ LNPs vaccine immunization protection against SARS-CoV-2 challenge in hamsters

The presence of infectious titers was determined by the $TCID_{50}$/ml method, and the results were expressed as $log10$ of viral particles per milliliter of lung tissue. The mean of the experimental data was analyzed using a one-way ANOVA. (*$P<0.05$, **$P<0.01$, ***$P<0.001$)

mRNA/LNPs: Messenger RNA/lipid nanoparticles, $TCID_{50}$: The 50% tissue culture infectious dose

While intramuscular vaccination resulted in significantly higher serum neutralizing antibody titers than intranasal vaccination (51.2 vs. 22.0, $P<0.01$), the intranasal route led to a greater reduction in lung viral load.

As shown in Figure 8, hamsters that received empty LNPs intramuscularly or intranasally showed high viral loads, with mean titers of approximately 5×10^5 and 1×10^5 $TCID_{50}$/mL, respectively, and no statistically significant difference between these two control groups ($P=0.23$), confirming that the empty vehicle does not confer protection by either route. In sharp contrast, animals immunized intramuscularly with 5 µg of mRNA-LNPs exhibited a dramatic reduction in viral titer to approximately 2×10^2 $TCID_{50}$/ml. Relative to the empty LNP IM control, this represents a reduction of more than 3.5 log_{10} units ($P<0.0001$). Notably, the group that received the same intranasal dose showed the greatest protection, with viral titers reduced to approximately 2×10^1 $TCID_{50}$/ml. Compared to the empty LNP IN control, the intranasal vaccine achieved an even greater reduction of nearly 4.5 log_{10} units ($P<0.0001$). Most importantly, the intranasal vaccine group exhibited significantly lower viral titers than the intramuscular vaccine group ($P=0.014$), representing an additional 1.6-log decrease. This difference is both statistically and biologically meaningful, as it placed the majority of IN-vaccinated animals at or near the limit of detection. In contrast, IM-vaccinated animals still had measurable residual virus. Evaluation of virus replication in lung tissue showed that intranasal mRNA-LNP administration conferred a 4-log reduction in viral load against SARS-CoV-2 challenge. Collectively, these findings indicate that both routes of mRNA-LNP vaccination significantly reduce viral replication in the lungs compared to controls. Still, intranasal immunization offers superior

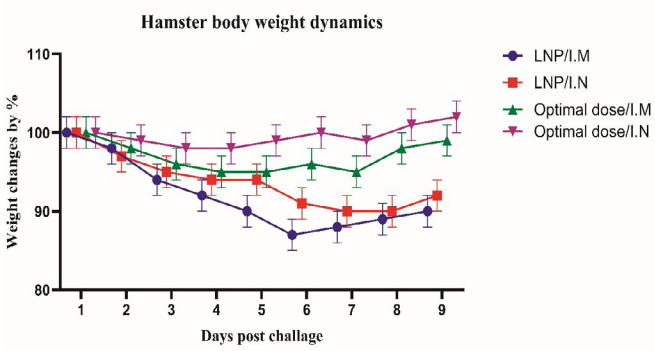

Figure 9. Mean percentage of weight change (error bars represent SEM) over 9 days after SARS-CoV-2 challenge in control and vaccinated hamsters SEM: Standard error of the mean, I.M: Intramuscular, I.N: Intranasal

protection, nearly eliminating detectable infectious virus. This highlights the added benefit of mucosal delivery for respiratory pathogens like SARS-CoV-2, likely due to stronger local immune responses at the site of infection.

Following the intranasal SARS-CoV-2 challenge, weight changes in the immunized hamsters were monitored for nine days post-infection (Figure 9). Hamsters that received empty LNPs intramuscularly exhibited the most significant weight loss (~10%), while those that received empty LNPs intranasally lost approximately 8% of their body weight. In contrast, the group immunized intramuscularly with 5 µg of mRNA-LNPs experienced only slight weight loss (~1%). Remarkably, the group immunized intranasally with the same vaccine dose showed a 2% weight gain. These results demonstrate that vaccination with 5 µg of mRNA-LNPs provided effective protection against SARS-CoV-2-induced weight loss, a clinical marker of disease severity in hamsters. The intranasal route conferred the most significant protection and prevented weight loss, suggesting robust mucosal and systemic immunity. In contrast, animals that received empty LNPs, regardless of the route, showed notable weight loss, confirming the absence of protective efficacy in the control groups.

Discussion

The respiratory mucosa is the primary site of entry for viral transmission and initial infection, the virus mainly replicates in the ciliated columnar epithelial cells of the upper respiratory tract (URT). Nasal-associated lymphoid tissue (NALT), found in the URT, recognizes inhaled antigens and serves as a first line of defense against respiratory viruses (28). As an inductive site for both humoral and cellular immunity, NALT is a valuable target for vaccines against respiratory viruses. Ideally, nano-vaccines should mimic the route of pulmonary infection to deliver antigens to the NALT mucosal tissue, triggering a selective mucosal immune response. Consequently, factors such as formulation, nanoparticle size, and antigen presentation play a critical role in the development of effective nano-vaccines targeted to the NALT (29).

Studies show that intranasal vaccination is more effective than subcutaneous or intramuscular immunization at generating mucosal immunity against respiratory viruses because it more closely resembles natural infection. The fact that it can be easily self-administered and could occupy a significant market share in the future adds to its benefits (30). Intranasal delivery is known to induce higher levels of antigen-specific lymphocyte proliferation, increased secretion of cytokines such as interferon-γ and interleukins, and the formation of antigen-specific IgA antibodies (31).

Interestingly, an inverse relationship between IgA and IgG responses has been observed during COVID-19 infection, meaning that a robust systemic IgG response to a vaccine does not necessarily imply a strong IgA response in mucosal areas (32). Therefore, individuals vaccinated systemically may still be susceptible to SARS-CoV-2 infection via the respiratory tract and may act as asymptomatic carriers due to comparatively weak mucosal immunity (33). Therefore, nasal vaccines have a strategic advantage in preventing diseases such as SARS-CoV-2, as they can be highly immunogenic and reduce viral shedding (27).

In this study, we observed the immunogenicity of a formulated mRNA vaccine delivered via LNPs. Our findings demonstrate that the developed vaccine induces high IgA levels in a mouse model. Additionally, the vaccine significantly limits SARS-CoV-2 viral multiplication in hamsters.

Conventional vaccines are used to prevent diseases caused by pathogens such as bacteria and viruses. However, there are challenges in manufacturing and distributing conventional vaccines at scale. mRNA-based vaccine constructs have demonstrated the ability to produce high levels of neutralizing antibodies in animal studies at low doses with only one or two administrations. Implementing the mRNA-LNP platform as a vaccine for emerging and re-emerging viruses could be a promising approach. For example, small animals and non-human primates (NHPs) immunized with an mRNA-LNP vaccine encoding the pre-membrane (prM) and envelope (E) glycoproteins of Zika virus showed high and long-lasting neutralizing antibody levels, providing sterilizing immunity against Zika infection (34, 35).

Similarly, animals immunized intramuscularly with an mRNA vaccine formulated in lipid nanoparticles (LNPs) encoding the rabies virus glycoprotein (RABV-G) developed protective antibody titers that could be boosted and remained stable for one year (36). With the increasing scrutiny of the long-term effects of mRNA mass vaccination during the COVID-19 pandemic, this platform is likely to become more dominant in developing vaccines for many viruses, such as rabies, seasonal influenza, Zika, and cytomegalovirus (CMV). However, besides SARS-CoV-2 and respiratory syncytial virus (RSV), none of these have progressed beyond clinical trials. This pandemic clearly shows the importance of technological platforms that enable rapid vaccine development and scalable manufacturing (37). The rapid development, large-scale production, and clinical use of mRNA-based vaccines during the COVID-19 pandemic serve as proof of concept that RNA-based vaccines represent a promising new strategy for immunization.

Seroconversion is the process by which a person develops detectable specific antibodies in their blood serum following infection or immunization. Seroprotection refers to the presence of antibody levels considered sufficient to protect against infection by a specific pathogen. In this study, hamsters immunized with 5 µg mRNA-LNPs, particularly via the intranasal route, demonstrated very low viral titers in lung tissues post-challenge (~10^1 $TCID_{50}$/mL), suggesting robust seroconversion, as the animals mounted effective immune responses prior to exposure. The high levels of neutralizing antibodies observed in earlier serum analyses

from the same vaccinated groups (as indicated by ELISA and VNT data) further confirm successful seroconversion. Moreover, the dramatic reduction in viral replication following challenge, especially in the intranasally immunized group, indicates that these antibody levels were not only present but functionally protective, thereby meeting the criteria for seroprotection. The minimal to no weight loss and superior viral clearance in these animals support the conclusion that the systemic and mucosal immunity elicited by the vaccine was sufficient to prevent significant disease and limit virus replication. The significant reduction in lung viral titers, especially in the group that received intranasal immunization, directly supports the vaccine's potential to reduce viral shedding and limit SARS-CoV-2 transmission. Furthermore, intranasal vaccination induces mucosal IgA antibodies in the respiratory tract, which can neutralize the virus at its point of entry, preventing the establishment and spread of infection.

While the present study selected the 5 μg dose for intranasal administration based on the optimal dose identified for the intramuscular route, we acknowledge that the dose-response relationship may differ for mucosal immunization. The optimal intranasal dose may be higher or lower due to differences in antigen uptake, local degradation, and immune cell targeting within the nasal-associated lymphoid tissue (NALT). Future dose-escalation studies specifically designed for the intranasal route are warranted to determine the optimal dose for mucosal immunity formally and to rule out potential dose-dependent tolerability issues.

Assessing Th2-associated cytokines, such as IL-4, and employing intracellular cytokine staining via flow cytometry would provide a more comprehensive understanding of the $CD4^+$ T cell polarization profile—specifically the Th1/Th2 balance—elicited by intranasal versus intramuscular vaccination. The present study focused on the Th1-biased IFNγ response as a well-established correlate of protection against viral challenge. Future investigations should incorporate multiparameter flow cytometry and measurement of Th2 cytokines (e.g., IL-4 and IL-5) to delineate further the cellular immune landscape induced by each route of administration.

It is important to clarify that the present study does not claim that intranasal vaccination is superior to the intramuscular route in eliciting systemic humoral or cellular immune responses. On the contrary, our data indicate that intramuscular administration tended to elicit higher serum levels of spikespecific IgG, stronger Th1biased IFNγ responses, and higher neutralizing antibody titers than the intranasal route. However, the primary objective of a mucosal vaccine is not necessarily to achieve superior systemic immunity, but rather to provide effective protection at the mucosal portal of viral entry. Our findings suggest that the intranasal route may offer certain advantages in terms of clinically relevant protective endpoints following viral challenge. Specifically, intranasal vaccination was associated with a significantly greater reduction in lung viral load (approximately 1.6log lower than that of the intramuscular group; $p = 0.014$). It appeared to confer more complete protection against weight loss, whereas intramuscularly vaccinated animals exhibited a mild but measurable reduction in body weight. These observations raise the possibility that, despite lower systemic antibody titers, the intranasal route may elicit local mucosal immune responses – potentially including spikespecific IgA in the respiratory tract – that help limit viral replication at the site of infection and mitigate clinical disease. Nevertheless, further studies are needed to establish the mechanistic basis for these differences directly and to confirm the generalizability of these findings. For respiratory pathogens such as SARSCoV2, the protective efficacy of a vaccine candidate may therefore benefit from evaluation not only of systemic immune correlates but also of local mucosal responses and the capacity to block viral establishment in the respiratory tract.

Thus, the correlation between serological responses (seroconversion and seroprotection) and virological outcomes (lung viral titers) underscores the efficacy of the mRNA-LNP vaccine, particularly via the intranasal route, in providing strong, protective immunity against SARS-CoV-2.

Conclusion

Given the high global burden of respiratory tract infections, there is a need for more effective interventional measures. Vaccination remains the best method for preventing respiratory virus infections. The mRNA platform, combined with lipid nanoparticles (LNPs), offers opportunities to address multiple unmet needs that traditional vaccines cannot meet. When administered intranasally, nano-vaccines enable easy, safe transport of the antigen to the NALT, thereby stimulating both mucosal and systemic immunity. Since IgA seroconversion occurs earlier with mRNA vaccination and involves mast cell activation, it is very important for controlling infection. This strategy may apply to other respiratory viruses and could be a feasible solution for future pandemics.

Acknowledgment

We thank all members of the Virology Department of Tarbiat Modares University, Tehran, Iran.

Funding

This work received support from Grant No. Med-523919, provided by the Research Deputy at Tarbiat Modares University, Faculty of Medical Sciences, Tehran, Iran.

Data Availability

All datasets used and/or analyzed during the current study are available from the corresponding author upon reasonable request.

Authors' Contributions

M A was responsible for study design, formal analysis, methodology, investigation, data curation, and both writing the original draft and reviewing and editing. H S contributed to conceptualization, study design, formal analysis, methodology, investigation, and data curation, and participated in writing the original draft and in review and editing. S S and A A were involved in study design, formal analysis, and methodology.

Conflicts of Interest

The authors declare no conflicts of interest.

Declaration

The authors confirm that this manuscript was prepared

without the use of any AI-assisted technologies or generative AI tools.

References

1. Jin J, Agarwala N, Kundu P, Harvey B, Zhang Y, Wallace E, Chatterjee N. Individual and community-level risk for COVID-19 mortality in the United States. Nat Med 2021;27:264-269.
2. Chen L, Liu W, Zhang Q, Xu K, Ye G, Wu W, *et al.* RNA based mNGS approach identifies a novel human coronavirus from two individual pneumonia cases in 2019 Wuhan outbreak. Emerg Microbes Infect 2020;9:313-319.
3. Teo SP. Review of COVID-19 mRNA Vaccines: BNT162b2 and mRNA-1273. J Pharm Pract 2022;35:947-951.
4. Du L, Yang Y, Zhou Y, Lu L, Li F, Jiang S. MERS-CoV spike protein: A key target for antivirals. Expert Opin Ther Targets 2017;21:131-143.
5. Ng WH, Liu X, Mahalingam S. Development of vaccines for SARS-CoV-2. F1000Res 2020;9: F1000 Faculty Rev-991.
6. Pollard AJ, Bijker EM. A guide to vaccinology: from basic principles to new developments. Nat Rev Immunol. 2021;21(2):83-100.
7. Verdecia M, Kokai-Kun JF, Kibbey M, Acharya S, Venema J, Atouf F. COVID-19 vaccine platforms: Delivering on a promise? Hum Vaccin Immunother 2021;17:2873-2893.
8. Fang E, Liu X, Li M, Zhang Z, Song L, Zhu B, *et al.* Advances in COVID-19 mRNA vaccine development. Signal Transduct Target Ther 2022;7:94.
9. Dhama K, Dhawan M, Tiwari R, Emran TB, Mitra S, Rabaan AA, *et al.* COVID-19 intranasal vaccines: current progress, advantages, prospects, and challenges. Hum Vaccin Immunother 2022;18:2045853.
10. Baldeon Vaca G, Meyer M, Cadete A, Hsiao CJ, Golding A, Jeon A, *et al.* Intranasal mRNA-LNP vaccination protects hamsters from SARS-CoV-2 infection. Sci Adv 2023;9:eadh1655.
11. Jackson NAC, Kester KE, Casimiro D, Gurunathan S, DeRos[illegible] F. The promise of mRNA vaccines: A biotech and industrial perspective. NPJ Vaccines 2020;5:11.
12. Mirtaleb MS, Falak R, Heshmatnia J, Bakhshandeh B, Taheri RA, Soleimanjahi H, Zolfaghari Emameh R. An insight overview on COVID-19 mRNA vaccines: Advantageous, pharmacology, mechanism of action, and prospective considerations. Int Immunopharmacol 2023;117:109934.
13. Crommelin DJA, Anchordoquy TJ, Volkin DB, Jiskoot W, Mastrobattista E. Addressing the cold reality of mRNA vaccine stability. J Pharm Sci 2021;110:997-1001.
14. Malone RW, Felgner PL, Verma IM. Cationic liposome-mediated RNA transfection. Proc Natl Acad Sci U S A 1989;86:6077-6081.
15. Kong W, Wei Y, Dong Z, Liu W, Zhao J, Huang Y, *et al.* Role of size, surface charge, and PEGylated lipids of lipid nanoparticles (LNPs) on intramuscular delivery of mRNA. J Nanobiotechnology 2024;22:553.
16. Reichmuth AM, Oberli MA, Jaklenec A, Langer R, Blankschtein D. mRNA vaccine delivery using lipid nanoparticles. Ther Deliv 2016;7:319-34.
17. Pascolo S. Synthetic messenger RNA-based vaccines: From scorn to hype. Viruses 2021;13:270.
18. Zamani P, Mashreghi M, Rezazade Bazaz M, Zargari S, Alizadeh F, Dorrigiv M, *et al.* Characterization of stability, safety and immunogenicity of the mRNA lipid nanoparticle vaccine Iribovax® against COVID-19 in nonhuman primates. J Control Release 2023;360:316-334.
19. Corbett KS, Edwards DK, Leist SR, Abiona OM, Boyoglu-Barnum S, Gillespie RA, *et al.* SARS-CoV-2 mRNA vaccine design enabled by prototype pathogen preparedness. Nature 2020;586:567-571.
20. Yahyaei S, Abdoli A, Jamali A, Teimoori A, Arefian E, Eftekhari Z, Jamur P. Targeting respiratory viruses: The efficacy of intranasal mrna vaccination in generating protective mucosal and systemic immunity against influenza a (H1N1). Influenza Other Respir Viruses 2025;19:e70093.
21. Zhuang X, Qi Y, Wang M, Yu N, Nan F, Zhang H, *et al.* mRNA vaccines encoding the HA protein of influenza A H1N1 virus delivered by cationic lipid nanoparticles induce protective immune responses in mice. Vaccines (Basel) 2020;8:123.
22. Freyn AW, Ramos da Silva J, Rosado VC, Bliss CM, Pine M, Mui BL, *et al.* A multi-targeting, nucleoside-modified mRNA influenza virus vaccine provides broad protection in mice. Mol Ther 2020;28:1569-1584.
23. Najafi N, Soleimanjahi H, Moghaddam-Banaem L, Raoufy MR, Shahali S, Kazemnejad A, Nasiri Z. Humoral immunogenicity assessment after receiving three types of SARS-CoV-2 vaccine. Sci Rep 2023;13:20213.
24. Reynolds SP, Edwards JH, Jones KP, Davies BH. Immunoglobulin and antibody levels in bronchoalveolar lavage fluid from symptomatic and asymptomatic pigeon breeders. Clin Exp Immunol 1991;86:278-285.
25. Shafaati M, Bagherzadeh K, Lotfinia M, Karimi H, Teimoori A, Razazian M, *et al.* The protection quest is a primary key to sharing the neutralizing antibody response to cover against all emerging VOCs based on BIV1-CovIran studies. Heliyon 2023;9:e14108.
26. Miller J, Ulrich R. On the analysis of psychometric functions: the Spearman-Kärber method. Percept Psychophys 2001;63:1399-1420.
27. Abdoli M, Shafaati M, Ghamsari LK, Abdoli A. Intranasal administration of cold-adapted live-attenuated SARS-CoV-2 candidate vaccine confers protection against SARS-CoV-2. Virus Res 2022;319:198857.
28. Kong H, Yan M, Yu Q, Yang Q. Characteristics of nasal-associated lymphoid tissue (NALT) and nasal absorption capacity in chicken. PLoS One 2013;8:e84097.
29. Hall K, Blair Zajdel ME, Blair GE. Unity and diversity in the human adenoviruses: exploiting alternative entry pathways for gene therapy. Biochem J 2010;431:321-336.
30. Canedo-Marroquín G, Saavedra F, Andrade CA, Berrios RV, Rodríguez-Guilarte L, Opazo MC, *et al.* SARS-CoV-2: Immune response elicited by infection and development of vaccines and treatments. Front Immunol 2020;11:569760.
31. McCormick AA, Shakeel A, Yi C, Kaur H, Mansour AM, Bakshi CS. Intranasal administration of a two-dose adjuvanted multi-antigen TMV-subunit conjugate vaccine fully protects mice against *Francisella tularensis* LVS challenge. PLoS One 2018;13:e0194614.
32. Butler SE, Crowley AR, Natarajan H, Xu S, Weiner JA, Lee J, *et al.* Features and functions of systemic and mucosal humoral immunity among SARS-CoV-2 convalescent individuals. medRxiv 2020; 2020.08.05.20168971.
33. Bleier BS, Ramanathan M, Jr., Lane AP. COVID-19 vaccines may not prevent nasal SARS-CoV-2 infection and asymptomatic transmission. Otolaryngol Head Neck Surg 2021;164:305-307.
34. Pardi N, Hogan MJ, Pelc RS, Muramatsu H, Andersen H, DeMaso CR, *et al.* Zika virus protection by a single low-dose nucleoside-modified mRNA vaccination. Nature 2017;543:248-51.
35. Richner JM, Himansu S, Dowd KA, Butler SL, Salazar V, Fox JM, *et al.* Modified mRNA vaccines protect against zika virus infection. Cell 2017;168:1114-25.e10.
36. Lutz J, Lazzaro S, Habbeddine M, Schmidt KE, Baumhof P, Mui BL, *et al.* Unmodified mRNA in LNPs constitutes a competitive technology for prophylactic vaccines. NPJ Vaccines 2017;2:29.
37. Alberer M, Gnad-Vogt U, Hong HS, Mehr KT, Backert L, Finak G, *et al.* Safety and immunogenicity of a mRNA rabies vaccine in healthy adults: An open-label, non-randomised, prospective, first-in-human phase 1 clinical trial. Lancet 2017;390:1511-1120.